MANEUVER DETECTION OF SPACE OBJECT FOR SPACE SURVEILLANCE

Jian Huang*, Weidong Hu, Lefeng Zhang

**ATR State Key Lab., National University of Defense Technology, Changsha, Hunan Province, China*
Email: huangjian@nudt.edu.cn

ABSTRACT

Maneuver detection is a very important task for maintaining the catalog of the orbital objects and space situational awareness. This paper mainly focuses on the typical maneuver scenario where space objects only perform tangential orbital maneuvers during a relative long gap. Particularly, only two classical and commonly applied orbital transition manners are considered, i.e. the twice tangential maneuvers at the apogee and the perigee or one tangential maneuver at an arbitrary time. Based on this, we preliminarily estimate the maneuvering mode and parameters by analyzing the change of semi-major axis and eccentricity. Furthermore, if only one tangential maneuver happened, we can formulate the estimation problem of maneuvering parameters as a non-linear least squares problem. To obtain a more sensible and accurate result, the prior knowledge is incorporated into the iterative solving process calculated by SOCP algorithm. Finally, the performance and efficiency of our method are validated by the theoretical analysis and some observations.

1 INTRUDUCTION

Nowadays, there are at least 20000 trackable objects in earth orbit and among them 1300 have the capability of performing orbital maneuver [1]. When the orbital maneuver occurs unexpectedly during the gaps, how to detect and reconstruct the abnormal event will directly affect the capability of space situational awareness. Particularly, the available observations collected by the current space surveillance systems, such as the AFSSS (US Air Force Space Surveillance System) [2], which has a long gap between the neighboring observations, are generally discrete in the spatial-temporal domain. The problem of maneuver detection during observation gaps brings much more difficult, in contrast with that commonly encountered in real-time tracking applications.

Regarding the problem of maneuver detection, the corresponding methods are the varieties with respect to different modes of orbital maneuvering and detection metrics. Storch estimated the maneuvering parameters of a collocated satellite in geosynchronous orbit by using nonlinear least squares [3]. In [4], the energy per unit mass was computed to detect a space event based on the technique of a moving window curve fit. Holzinger & Scheeres presented an object correlation and maneuver detection method using optimal control performance metrics [5]. Kelecy & Jah focused on the detection and reconstruction of single low thrust in-track maneuvers by using the orbit determination strategies based on the batch least-squares and extended Kalman filter (EKF) [6]. However, these methods are highly relevant to the presupposed maneuvering mode and a relative short observation gap.

In this paper, to address the real observed data, we only consider the common maneuvering modes and observation scenarios in practical. For an orbital maneuver, minimization of fuel consumption is essential because the weight of a payload that can be carried to the desired orbit depends on this minimization. Therefore, choices in the modes of orbital maneuver are limited. The thrust imposed on the tangential direction is an efficient maneuvering mode for minimizing fuel consumption, which is commonly applied in the process of various orbital maneuvers [7]. In particular, the maneuvering positions are usually chosen at the apogee and perigee point [7]. The studies in this paper are based on all the above-mentioned hypothetical maneuvering modes. Furthermore, due to the limited coverage of the sensors, the small and regular observation gap couldn't be guaranteed, which may be from hours to many days. Therefore, it is more meaningful and expected that the performance of the proposed maneuver detection method will be little affected by the observation gap, especially the large gap. Certainly, we also hope to reconstruct the maneuvering parameters precisely when the maneuver event occurs during a small gap.

This paper presents a novel and stepwise algorithm to handle these problems as follows. In section 2, the maneuvering modes and maneuvering parameters are estimated preliminarily according to the change of semi-major axis and eccentricity. If there is only one tangential maneuver during the gap from the result, we formulate the estimation problem of maneuvering parameters as a non-linear least squares problem. Thus, a more precise result can be obtained by solving the constrained non-linear least squares iterative process using SOCP (Second Order Cone Programming) algorithm in Section3. Section 4 is the simulation

results and performance analysis. Section 5 is the conclusion.

2 ESTIMATION OF MANEUVERING MODE

As we know, the orbits often have the unexpectable changes due to undertaking the various tasks. The most frequent orbital maneuvers are implemented to keep the spacecraft at the prearranged orbit, especially the semi-major axis a and eccentricity e which determine the orbital shape. Generally, these two orbital parameters are controlled more rigorously than any other parameters, and they are usually not allowed to fluctuate with respect to the time. The common and efficient maneuvering mode is to exert an additional tangential velocity at a proper point or the perigee and apogee point [7]. However, one tangential maneuver can't simultaneously adjust the semi-major axis and eccentricity arbitrarily, while two tangential maenuvers at the apogee and perigee can do that. They are both the common applying maneuvering modes. Therefore, the maneuvering mode and the corresponding maneuvering parameters can be estimated preliminarily according to the change of semi-major axis and eccentricity.

2.1 One tangential maneuvering mode

If the observed semi-major axis and eccentricities changed obviously at different times, the maneuver detection should be taken into account. Based on the hypothesis of one tangential maneuvering mode, we should reconstruct the maneuvering velocity as well as judge that where the maneuver occurs and whether only one tangential maneuver can realize this change of these parameters.

According to the perturbation motional formula, a tangential impulse velocity Δv exerted at an arbitrary point f during the orbit will simultaneously change the value of the semi-major axis Δa and eccentricity Δe as Eq. 1:

$$\begin{cases} \Delta a = \dfrac{2}{n\sqrt{1-e^2}}\left(1+2e\cos f+e^2\right)^{1/2}\Delta v \\ \Delta e = \dfrac{2\sqrt{1-e^2}}{na}\left(1+2e\cos f+e^2\right)^{-1/2}\left(\cos f+e\right)\Delta v \end{cases} \tag{1}$$

Where $n=\sqrt{\mu/a^3}$, $\mu = 3.98600436\times10^{14}\,m^3/s^2$ is the earth gravitational constant, f is the true anomaly. Once the Δa and Δe are known, we can calculate the maneuvering parameters f and Δv. Dividing the second equation by the first equation at Eq. 1, we can obtain that:

$$\cos f = \frac{\Delta a\left(e^3-e\right)+\Delta e\left(a+ae^2\right)}{\Delta a\left(1-e^2\right)-2ae\Delta e} \tag{2}$$

When we want to obtain the sensible values of the maneuvering true anomaly f and velocity Δv, the solution of Eq. 2 must satisfy:

$$-1\le\cos f\le 1 \tag{3}$$

However, Eq. 3 can't be always satisfied, i.e. only one tangential maneuver can't simultaneously adjust the semi-major axis and eccentricity arbitrarily. Therefore, multiple maneuvers should be applied, one efficient mode of which is that twice tangential maneuvers at the apogee and perigee point which could minimize the fuel consumption.

2.2 Twice tangential maneuvers at the perigee and apogee

Most of the orbits of space objects have small eccentricities and can be approximated as circle orbits. Thus, the item e^2 in Eq. 1 can be omitted. Eq. 1 can be transformed into:

$$\begin{cases} n\Delta a = -2\left(1+2e\cos f+e^2\right)^{1/2}\Delta v \\ na\Delta e = -2\left(1+2e\cos f+e^2\right)^{-1/2}\left(\cos f+e\right)\Delta v \end{cases} \tag{4}$$

Firstly, the Δv is used to adjust the eccentricity e at the perigee or the apogee, i.e. $f=0^\circ$ or $f=180^\circ$. This maneuvering velocity is denoted as $(\Delta v)_e$.

When $f=0^\circ$, we can get $(\Delta v)_e=(na\Delta e)/2$. When $f=180^\circ$, $(\Delta v)_e=-(na\Delta e)/2$.

After the adjusting of eccentricity e, the semi-major axis a should be modified a value Δa^* to adapt the final change. Δa^* includes two parts: the first is original changed value Δa; the second is the deviation $-(\mathrm{d}a)_e$ caused by the adjusting of e. Thus, the current value is $\Delta a^*=\Delta a-(\mathrm{d}a)_e$. Therefore, when $f=0^\circ$, $\Delta a^*=\Delta a+(-e-1)a\Delta e$; when $f=180^\circ$, $\Delta a^*=\Delta a+(e-1)a\Delta e$. In addition, when the signs of Δa and Δe are the same, we choose $f=0^\circ$; while they are different, we choose $f=180^\circ$. Accordingly, the value of Δa^* will be reduced and the fuel consumption is saved.

In order to adjust the Δa^*, we exert an equivalent tangential velocity $(\Delta v)_a^*$ each once at the apogee and perigee respectively. In this case, the eccentricity e will not be changed while adjusting a according to Eq. 4. We can obtain that $(\Delta v)_a^*=(n\Delta a^*)/4$. Finally,

twice tangential maneuvers at the perigee and apogee can be utilized to achieve the arbitrary change of eccentricity e and the semi-major axis a. The concrete formats are as follows:

(1) When the sign of Δa and Δe are the same, $\Delta a^* = \Delta a - (1+e)a\Delta e$, and the first tangential impulse Δv_1 is exerted at $f = 0^\circ$, the second tangential impulse Δv_2 is exerted at $f = 180^\circ$, where

$$\begin{cases} \Delta v_1 = \dfrac{na\Delta e}{2} + \dfrac{n\Delta a^*}{4} = n\dfrac{\Delta a + (1-e)a\Delta e}{4} \\ \Delta v_2 = \dfrac{n\Delta a^*}{4} = n\dfrac{\Delta a - (1+e)a\Delta e}{4} \end{cases} \tag{5}$$

(2) When the sign of Δa and Δe are different, $\Delta a^* = \Delta a - (1-e)a\Delta e$, and the first tangential impulse Δv_1 is exerted at $f = 180^\circ$, the second tangential impulse Δv_2 is exerted at $f = 0^\circ$, where

$$\begin{cases} \Delta v_1 = -\dfrac{na\Delta e}{2} + \dfrac{n\Delta a^*}{4} = n\dfrac{\Delta a - (1+e)a\Delta e}{4} \\ \Delta v_2 = \dfrac{n\Delta a^*}{4} = n\dfrac{\Delta a - (1-e)a\Delta e}{4} \end{cases} \tag{6}$$

Therefore, the common maneuvering modes for adjusting the eccentricity e and the semi-major axis a have been introduced. When we get the observations at different time, the maneuvering mode and parameters can be reconstructed according to the value of Δa and Δe. Then, the sensibility and availability of the results can be further analyzed.

2.3 Analysis of observed data

To verify the effectiveness of our presented maneuver detection method, some typical orbital observations of Shenzhou Spaceship are selected for maneuver detection.

The observations are displayed in the form of the orbital period, i.e. the times of full circle where the space object turns around the observation station. The first data contains a neighbouring observation, and only the concerned altitude and eccentricity are plotted in Fig. 1.

We take the aforementioned two maneuvering modes to analyze the first observed data. The results are listed in Tab. 1, where X denotes no solution; Mode 1 and Mode 2 represent the one tangential maneuvee and twice tangential maneuvers at the perigee and apogee, respectively.

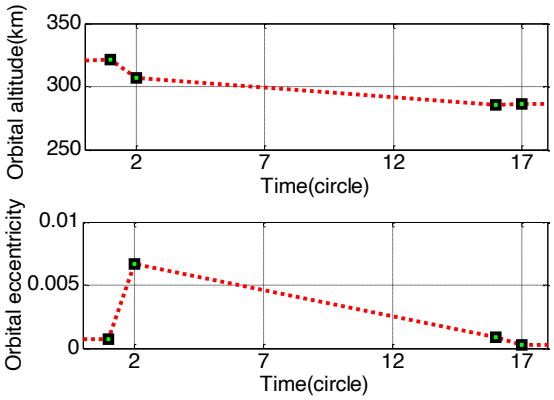

Figure 1. Observations at the first time

Table 1. Analysis results of the first observations

	Circle 1 to Circle 2		Circle 2 to Circle 16	
	Maneuver velocity (m/s)	Maneuver position f(°)	Maneuver velocity (m/s)	Maneuver position f(°)
Mode 1	X	X	X	X
Mode 2	-15.5	180	-17.4	0
	-15.5	0	3.9	180

From Tab. 1, we can see that the change of observed orbits from circle 1 to circle 2 can be achieved by exerting one -15.5m/s maneuvering velocity at the apogee and perigee respectively, while only one tangential maneuver can never realize it. For the second maneuver from circle 2 to circle 16, it can be realized by exerting a -17.4m/s impulse velocity at the perigee and then a 3.9m/s impulse at the apogee. In addition, the mode 1 still has no solution. Commonly, it is impossible that the velocity is reduced firstly, and then increased immediately. The second increase of velocity may be induced by the observation noise. Thus, the second maneuver can be equivalent to one tangential maneuver with about -15m/s impulse velocity. Therefore, the preliminary analysis result can be derived: there may be three times continual maneuvers at the perigee and apogee points. In addition, the tangential impulse velocity exerted at each time is about -15m/s.

The second observations are shown in Fig. 2.

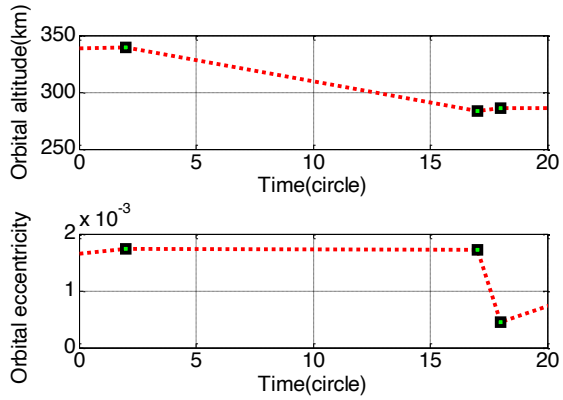

Figure 2. Observations at the second time

The same maneuver detection method is implemented to analyze the second observations. The results are shown in Tab. 2.

Table 2. Analysis results of the second observations

	Circle 2 to Circle 17		Circle 17 to Circle 18	
	Maneuver velocity (m/s)	Maneuver position f(°)	Maneuver velocity (m/s)	Maneuver position f(°)
Mode 1	-31.96	90.04	X	X
Mode 2	-15.99	0	3.30	180
	-15.96	180	3.29	0

The two maneuvering modes are both available to conform with the observations from circle 2 to circle 17. The maneuvering velocity in mode 1 is about the total of twice maneuvering velocities in mode 2. However, the thrusters should not always change the magnitude of impulse while concerning the stableness and difficulty of control and manufacture. So, the maneuvering velocity in mode 2 more approximates the analysis results of the first observations and may be sensible. In addition, the observations from circle 17 to circle 18 are inclined to suggest that no maneuver occurs during the gap, and the nonzero values of the estimated maneuvering velocity mainly results in the measurement error.

The analysis results of the observations indicate that our estimation method of the maneuvering mode is efficient. It can preliminarily deduce the maneuvering parameters and explicate sensibly for the observations. A further advantage is that the algorithm is little affected by the observation gap which ranges from 2 hours to 24 hours in our testing data. In addition, the method is straightforward. Even for the preliminary orbits determined based on the coarse observations, a robust and relative accurate result can be also obtained.

3 PRECISE ESTIMATION OF MANEUVERING PARAMETERS IN ONE TANGENTIAL MANEUVERING MODE

If the estimated maneuvering mode indicates that only one tangential impulse is exerted during the observation gap, we could reconstruct the maneuvering parameters more precisely.

3.1 Method of parameter estimation in orbital maneuvering

Let t_m and Δv denote the maneuvering time and velocity respectively. $\boldsymbol{v}_m$ and $\boldsymbol{v}'_m$ are the pre-maneuver velocity vector and the post-maneuver velocity vector at the time t_m, respectively. The space object maneuvers along the tangential direction, so we can derive $\boldsymbol{v}'_m = \boldsymbol{v}_m + \Delta v \bullet \boldsymbol{v}_m / v_m$, where $v_m = \|\boldsymbol{v}_m\|_2$, $\|\bullet\|_2$ denotes the ℓ_2-norm. $\boldsymbol{r}_0$, $\boldsymbol{v}_0$ and $\boldsymbol{r}_1$, $\boldsymbol{v}_1$ are the position vector and velocity vector of space object at the time t_0 and t_1, respectively. f_1, g_1, $\dot{f}_1$, $\dot{g}_1$ are the functions of $\boldsymbol{r}_0$, $\boldsymbol{v}_0$ and $t_m - t_0$. f_2, g_2, $\dot{f}_2$, $\dot{g}_2$ are the functions of $\boldsymbol{r}_m$, $\boldsymbol{v}'_m$ and $t_1 - t_m$ [8]. Assuming that the observation noise is zero mean Gaussian white noise, $\boldsymbol{n}(0, Q_0)$ and $\boldsymbol{n}(0, Q_1)$ denote the observation noises at the time t_0 and t_1, respectively, where Q_0 and Q_1 are the noise covariance.

Let $Q_0 = Q_1 = diag\left[\sigma_r^2, \sigma_r^2, \sigma_r^2, \sigma_v^2, \sigma_v^2, \sigma_v^2\right]$ in this paper. Thus, the observed orbital elements in the presence of noise is denoted by $\left[\boldsymbol{r}_0'^T, \boldsymbol{v}_0'^T\right]^T = \left[\boldsymbol{r}_0^T, \boldsymbol{v}_0^T\right]^T + \boldsymbol{n}(0, Q_0)$, $\left[\boldsymbol{r}_1'^T, \boldsymbol{v}_1'^T\right]^T = \left[\boldsymbol{r}_1^T, \boldsymbol{v}_1^T\right]^T + \boldsymbol{n}(0, Q_1)$.

The orbital maneuvering process can be represented by the following equation:

$$\begin{cases} \begin{bmatrix} \boldsymbol{r}_1' \\ \boldsymbol{v}_1' \end{bmatrix} = \begin{bmatrix} \boldsymbol{r}_1 \\ \boldsymbol{v}_1 \end{bmatrix} + \boldsymbol{n}(0, Q_1) = \\ \begin{bmatrix} f_2 \boldsymbol{I} & g_2 \boldsymbol{I} \\ \dot{f}_2 \boldsymbol{I} & \dot{g}_2 \boldsymbol{I} \end{bmatrix} \left(\begin{bmatrix} f_1 \boldsymbol{I} & g_1 \boldsymbol{I} \\ \dot{f}_1 \boldsymbol{I} & \dot{g}_1 \boldsymbol{I} \end{bmatrix} \begin{bmatrix} \boldsymbol{r}_0 \\ \boldsymbol{v}_0 \end{bmatrix} + \begin{bmatrix} 0 \\ \Delta v \bullet \boldsymbol{v}_m / v_m \end{bmatrix} \right) + \boldsymbol{n}(0, Q_1) \\ \begin{bmatrix} \boldsymbol{r}_0' \\ \boldsymbol{v}_0' \end{bmatrix} = \begin{bmatrix} \boldsymbol{r}_0 \\ \boldsymbol{v}_0 \end{bmatrix} + \boldsymbol{n}(0, Q_0) \end{cases} \tag{7}$$

where $\begin{bmatrix} \boldsymbol{r}_m \\ \boldsymbol{v}_m \end{bmatrix} = \begin{bmatrix} f_1 \boldsymbol{I} & g_1 \boldsymbol{I} \\ \dot{f}_1 \boldsymbol{I} & \dot{g}_1 \boldsymbol{I} \end{bmatrix} \begin{bmatrix} \boldsymbol{r}_0 \\ \boldsymbol{v}_0 \end{bmatrix}$. Here, the perturbation forces are not considered.

The first equation in the maneuvering model of Eq. 7 is abbreviated to $\begin{bmatrix} \boldsymbol{r}_1' \\ \boldsymbol{v}_1' \end{bmatrix} = \boldsymbol{\Phi}(\boldsymbol{r}_0, \boldsymbol{v}_0, \Delta v, t_m) + \boldsymbol{n}(0, Q_1)$.

Therefore, the parameter estimation problem can be treated as a non-linear least square problem in Eq. 8:

$$[\Delta \hat{v}, \hat{t}_m] = \arg\min_{\Delta v, t_m} \left(\begin{bmatrix} \boldsymbol{r}_1' \\ \boldsymbol{v}_1' \end{bmatrix} - \boldsymbol{\Phi}(\boldsymbol{r}_0, \boldsymbol{v}_0, \Delta v, t_m) \right)^T Q_1^{-1} \left(\begin{bmatrix} \boldsymbol{r}_1' \\ \boldsymbol{v}_1' \end{bmatrix} - \boldsymbol{\Phi}(\boldsymbol{r}_0, \boldsymbol{v}_0, \Delta v, t_m) \right) \tag{8}$$

where the unknown parameter vector is $\boldsymbol{\xi} = \left[\boldsymbol{r}_0, \boldsymbol{v}_0, \Delta v, t_m\right]^T$. Before the Gauss-Newton iterative algorithm being applied, we need compute the linearization form of $\boldsymbol{\Phi}(\boldsymbol{r}_0, \boldsymbol{v}_0, \Delta v, t_m)$ at the parameter vector $\boldsymbol{\xi}$:

$$\boldsymbol{H}(\boldsymbol{\xi}) = \left[\boldsymbol{H}(\boldsymbol{r}_0), \boldsymbol{H}(\boldsymbol{v}_0), \boldsymbol{H}(\Delta v), \boldsymbol{H}(t_m)\right] = \left[\frac{\partial \boldsymbol{\Phi}}{\partial \boldsymbol{r}_0}, \frac{\partial \boldsymbol{\Phi}}{\partial \boldsymbol{v}_0}, \frac{\partial \boldsymbol{\Phi}}{\partial \Delta v}, \frac{\partial \boldsymbol{\Phi}}{\partial t_m}\right] \tag{9}$$

The calculation of partial derivatives has no difficulty but is complicated, so we don't give the concrete forms due to the limited length of paper.

The initial value $\boldsymbol{\xi}(0)$ of the parameter vector $\boldsymbol{\xi}$ directly affects the convergence of the iterative algorithm. It is important to choose an appropriate initial value based on the prior information of the correlated orbits. In this paper, the observed values of $\boldsymbol{r}_0'$, $\boldsymbol{v}_0'$ at the time t_0 can be taken as the initial values of $\boldsymbol{r}_0$, $\boldsymbol{v}_0$. Moreover, let the observed orbit a and orbit b propagate in the time interval $[t_0, t_1]$. We calculate the intersection time t_m' when the two orbits have the minimum module difference of the position vectors through cross propagation. Thus, t_m' is chosen as the initial iterative value of t_m, and the corresponding module value $\Delta v'$ of the two velocity vectors' difference at the intersection point is chosen as the initial value of maneuvering velocity Δv.

In order to obtain a more sensible and accurate result, the constraints for the unknown parameter vector $\boldsymbol{\xi}$ should be applied in the iterative process. The constrained iterative form for solving the non-linear least squares problem is:

$$\boldsymbol{\xi}(n+1) = \arg\min_{\hat{\boldsymbol{\xi}}(n+1)} \left(\begin{bmatrix} \boldsymbol{r}_1' \\ \boldsymbol{v}_1' \end{bmatrix} - \boldsymbol{\Phi}(\boldsymbol{\xi}(n)) + \boldsymbol{H}(\boldsymbol{\xi}(n)) \left[\boldsymbol{\xi}(n) - \hat{\boldsymbol{\xi}}(n+1 \right. \right.$$
$$\left. \left. \cdot Q_1^{-1} \left(\begin{bmatrix} \boldsymbol{r}_1' \\ \boldsymbol{v}_1' \end{bmatrix} - \boldsymbol{\Phi}(\boldsymbol{\xi}(n)) + \boldsymbol{H}(\boldsymbol{\xi}(n)) \left[\boldsymbol{\xi}(n) - \hat{\boldsymbol{\xi}}(n+1) \right] \right) \right.$$

$$\text{s.t.} \begin{cases} \left\| \begin{bmatrix} \boldsymbol{r}_0(n+1) \\ \boldsymbol{v}_0(n+1) \end{bmatrix} - \begin{bmatrix} \boldsymbol{r}_0' \\ \boldsymbol{v}_0' \end{bmatrix} \right\| \le \begin{bmatrix} 3\sigma_r \mathbf{1}_3 \\ 3\sigma_v \mathbf{1}_3 \end{bmatrix} \\ 0 \le \Delta v(n+1) \le \Delta v_{\max} \\ t_0 \le t_m(n+1) \le t_1 \end{cases} \tag{10}$$

where $\Delta v_{\max}$ is the upper bound of the maneuvering velocity, $\mathbf{1}_3$ is a 3-dimensional full-1 vector. The iterative process is an optimization problem, which can be handled by the SOCP algorithm [9]. Therefore, the maneuvering time $\hat{t}_m$ and the maneuvering velocity $\Delta \hat{v}$ can be estimated by multiple iterations.

3.2 Detection performance of orbital maneuver

Using Eq. 9, $\partial \boldsymbol{r}_0 / \partial \boldsymbol{\xi}$ and $\partial \boldsymbol{v}_0 / \partial \boldsymbol{\xi}$, we can easily obtain the Cramer-Rao Lower Bound (CRLB) of the estimated parameters t_m and Δv. Here, two common gaps of the observations are used for the performance analysis, i.e.: one case is that the surveillance system observes two adjacent orbits of an object, whose time interval is about an orbital period (about 2 hours for LEO object); the other case is that the neighbouring ascending and descending arcs are observed, whose time interval is about 12 hours. In this paper, the simulation parameters are set as follows: the initial orbit element: Semi-major axis $a = 7000km$, Eccentricity $e = 0.01$, Inclination $i = 70^\circ$, Longitude of the ascending node $\Omega = 170^\circ$, Argument of periapsis $\omega = 30^\circ$, Mean anomaly $M = 30^\circ$; the observation errors are $\sigma_r = 10m$ and $\sigma_v = 0.1m/s$. Subsequently, we calculate the CRLBs in the simulation. For the non-maneuvering object, the CRLB's square root of the maneuvering velocity is 0.1m/s, which is similar to the observation error. For the maneuvering objects, the distribution of the CRLBs' square root of the estimated maneuvering time and maneuvering velocity are shown in Fig. 3.

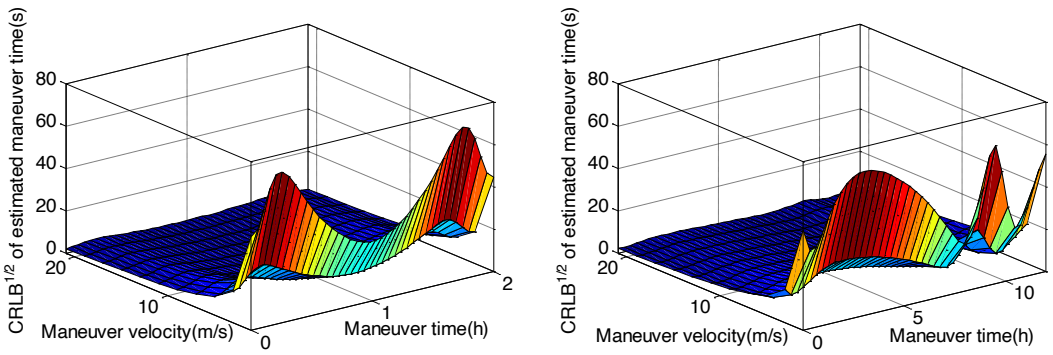

(a) The CRLBs' square root of the estimated maneuvering time

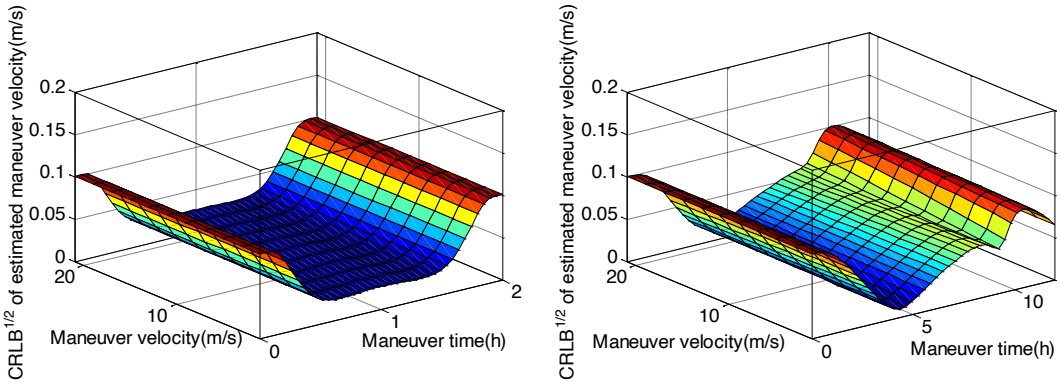

(b) The CRLBs' square root of the estimated maneuvering velocity

Figure 3. The distribution of the CRLBs' square root of the estimated maneuvering time and velocity

Fig. 3 indicates that the estimated precision fluctuates with respect to the maneuvering time instead of changing monotonously. With the increasing maneuvering velocity, the parameters will be estimated with a higher precision. In addition, the estimation precision for a large gap $t_1 - t_0$ of the observations is slightly higher than that for a small one.

Furthermore, Monte Carlo simulations are carried out to examine and analyze the maneuver detection performance and parameter estimation precision of the proposed algorithm. The result is compared with CRLB. The parameters in the simulation are the same with aforementioned setting.

Firstly, we carry out the maneuver detection for the non-maneuver object. The cumulative probability distribution of the estimated maneuver velocity is statistically shown in Tab. 3.

Table 3. The cumulative probability distribution of the estimated maneuvering velocity for the non-maneuvering object

Estimated maneuvering velocity (m/s)	$\leq 10^{-3}$	$\leq 10^{-2}$	≤ 0.1	≤ 0.3	≤ 0.6
Cumulative probability (2h)	0.4500	0.4550	0.6500	0.9450	1
Cumulative probability (12h)	0.5050	0.5250	0.7000	0.9950	1

Tab. 3 indicates that almost all the estimated maneuvering velocities are less than $3\sigma_v$, which result from the observations error. In other words, there is quite a small probability that a non-maneuver object is identified as a maneuver one.

Subsequently, the maneuver detection is carried out for the maneuver object. In this paper, when the estimation biases satisfy $\delta(t_m) \leq 60s$, $\delta(\Delta v) \leq 0.3m/s$, we assume that the orbital maneuver detection is correct. Only the correct maneuver detection is used to evaluate the accuracy of the parameter estimation. The result is shown in Fig. 4.

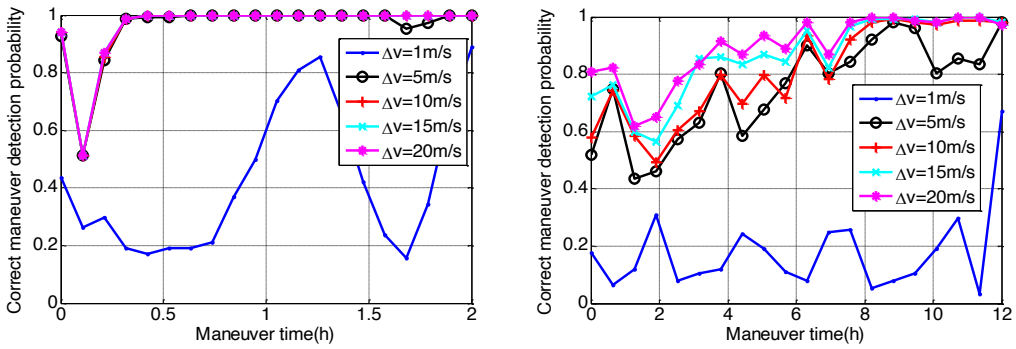

(a) Probability of correct maneuver detection

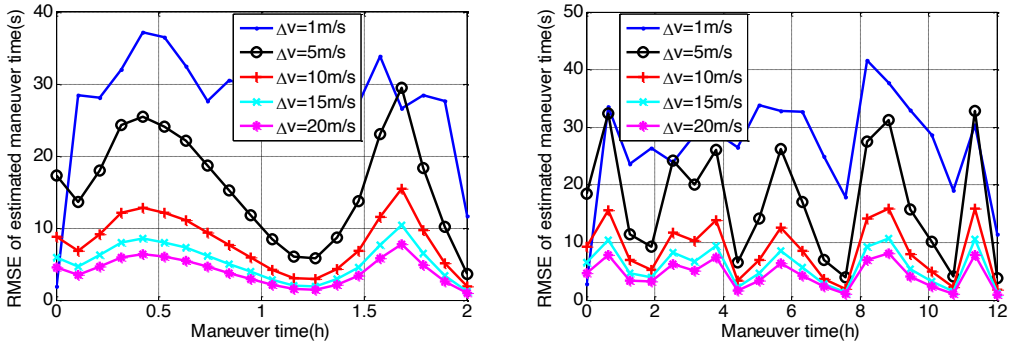

(b) Root Mean Square Error (RMSE) of the estimated maneuvering time

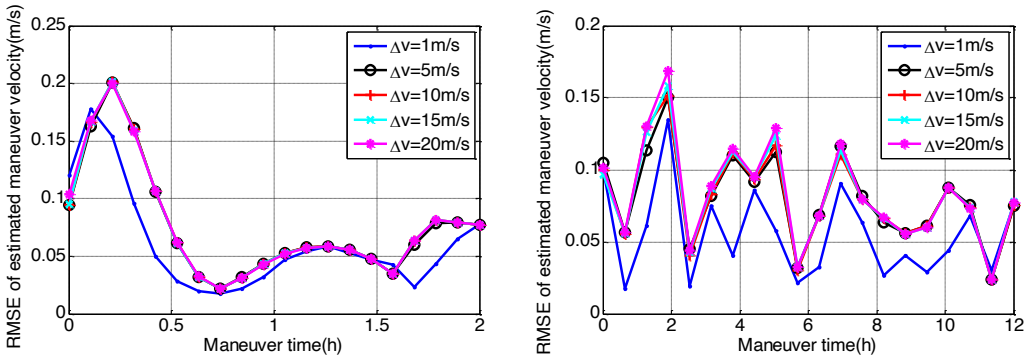

(c) Root Mean Square Error (RMSE) of the estimated maneuvering velocity

Figure 4. The detection performance of the proposed maneuver detection algorithm

Fig. 4 suggests that the detection performance is closely related with the real maneuvering time and the maneuvering velocity. Comparing the simulation results with the CRLBs, we can find that it will acquire a high correct detection probability where the CRLBs of the maneuvering time and velocity are low. When the maneuvering velocity exceeds 5m/s, the correct maneuvering detection probability can achieve 1. With the increasing maneuvering velocity, the estimation accuracy of the maneuvering time is improved. But the estimation accuracy of the maneuvering velocity is more sensitive to the real maneuvering time, which coincides with the trend of the CRLB. In addition, Fig. 4 also shows that the larger gap interval of the observations leads to a higher estimation accuracy than the smaller one, but the correct detection probability is much lower. The reasons behind this outcome are that it is much more difficult to get an accurate initial iterative value in the case of the large gap interval than the small gap. The larger difference between the initial iterative value and the real value will result in a higher probability of the non-convergence and local convergence problem. This is a main reason why the larger gap of the observations makes the orbital maneuver detection more difficult.

4 Conclusions

Maneuver detection plays an important role in space surveillance. This paper presents a novel method for addressing the maneuver detection problem under the hypothesis that only the tangential maneuvers exist. We preliminarily estimate the maneuvering mode according to the changes of the observed semi-major axis and eccentricity. This method is very convenient to handle the practical data and will be little affected by the observation gap. Some typical observations are used to verify the robust and efficiency of our presented algorithm. If estimated maneuvering mode shows that only one tangential maneuver occurs during the gap, the reconstruction problem of the maneuvering parameters can be transformed into a non-linear least squares problem. To obtain a stable and precise result of the least squares problem, some prior constrains are incorporated into the iterative processes. The SOCP algorithm is utilized to calculate the optimal problem. Finally, the performance of the proposed method is also analyzed in detail, and extensive simulations are carried out to validate the effectiveness of the algorithm. However, the proposed algorithm is a general methodology, which can be also adapted and extended to many different situations.

5 Reference

[1] James, L. (2009). On keeping the space

environment safe for civil and commercial users. *Before the Subcommittee on Space and Aeronautics, House Committee on Science and Technology*.

[2] Schumacher, P.W. &Jr. (2009). US navel space surveillance upgrade program 1999-2003. *Fifth European Conference on Space Debris, Darmstadt, Germany: ESA/ESOC*.

[3] Storch, T.R. (2005). *Maneuver estimation model for relative orbit determination*. Air Force Institute of Technology Wright-Patterson AFB OH School of Engineering And Management Air Force Institute of Technology, Ohio, Master thesis.

[4] Patera, R.P. (2008). Space event detection method. *Journal of Spacecraft and Rockets*, 45(3), 554-559.

[5] Holzinger, M.J. & Scheeres, D.J. (2010). Object correlation and maneuver detection using optimal control performance metrics. *Proceedings of the Advanced Maui Optical and Space Surveillance Technologies Conference*, Hawaii.

[6] Kelecy, T. & Jah, M. (2010). Detection and orbit determination of a satellite executing low thrust maneuvers. *Acta Astronautica*, 66, 798-809.

[7] Sidi, M.J. (1997). *Spacecraft dynamics and control: A practical engineering approach*. Cambridge University Press.

[8] Der, G.J. (1997). An elegant state transition matrix. *Journal of the Astronautical Sciences*, 45(4), 371-390.

[9] Lobo, M., Vandenberghe, L., Boyd, S, et al. (1998). Applications of the second-order cone programming. *Linear Algebra and its Appication*, 284: 193-228.